

# UC Berkeley

## Research Reports

### Title

Experimental Study Of Chatter Free Sliding Mode Control For Lateral Control Of Commuter Buses In AHS

### Permalink

<https://escholarship.org/uc/item/8d5462dk>

### Authors

Hingwe, Pushkar  
Tomizuka, Masayoshi

### Publication Date

1996

**This paper has been mechanically scanned. Some errors may have been inadvertently introduced.**

**CALIFORNIA PATH PROGRAM  
INSTITUTE OF TRANSPORTATION STUDIES  
UNIVERSITY OF CALIFORNIA, BERKELEY**

# **Experimental Study of Chatter Free Sliding Mode Control for Lateral Control of Commuter Buses in AHS**

**Pushkar Hingwe  
Masayoshi Tomizuka**  
*University of California, Berkeley*

**California PATH Research Report  
UCB-ITS-PRR-96-31**

This work was performed as part of the California PATH Program of the University of California, in cooperation with the State of California Business, Transportation, and Housing Agency, Department of Transportation; and the United States Department of Transportation, Federal Highway Administration.

The contents of this report reflect the views of the authors who are responsible for the facts and the accuracy of the data presented herein. The contents do not necessarily reflect the official views or policies of the State of California. This report does not constitute a standard, specification, or regulation.

November 1996

ISSN 1055-1425

# Experimental Study of Chatter Free Sliding Mode Control for Lateral Control of Commuter Buses in AHS

Pushkar Hingwe

Masayoshi Tomizuka

California Partners for Advanced Transit and Highways (PATH)

Mechanical Engineering Department

University of California at Berkeley March 1995

**Abstract** This report presents design and experimental evaluation of lateral controllers for commuter buses based on Sliding Mode Control (SMC). The objective of the control is to track the lane centerline. A nonlinear control strategy is needed to take care of variation in longitudinal velocity. SMC, a robust control technique, is selected because of passenger load uncertainties and variations in road tire interaction. Importance is given to reduction or elimination of the control chatter inherent in the SMC systems involving switching functions. Two SMC based controllers are designed and are shown to differ only in the position of an integrator which gets naturally introduced into the closed loop. One of the methods is chosen for experimental verification because it guarantees asymptotic tracking with no chatter in the control input to the steering actuator of the vehicle. At the time of writing this report no experimental bus was available, therefore close loop experiments done on a passenger car (Pontiac 6000) are presented.

**Keywords:** Advanced Vehicle Control Systems, Sliding Mode Control, Chatter reduction. Lateral control.

## Executive Summary

This report summarizes the second year research results on lateral control of Commuter Buses in Automated Highway Systems (AHS) conducted in the PATH project (MOU129) : Steering and Braking Control of Heavy Duty Vehicles. Lateral control of vehicles in the light of Intelligent Transportation Systems (ITS) and Automated Highway Systems (AHS) has been an active research subject in recent years. Though much of the work in the past has been concentrated in the area of light vehicles, a study done by Tsao (1995) regarding the deployment of AHS suggests that commuter buses may become prime candidates for the initial deployment of AHS. This is one of the motivations for the present study. This report is a continuation of the previous report (Hingwe and Tomizuka 1995) in which the application of Sliding Mode Control (SMC) methodology, a robust nonlinear control design technique, was studied in the context of lateral control of commuter buses. Two SMC based controllers were studied. For continuity, a brief summary of the SMCs is presented. Only lateral and yaw dynamics of the buses are considered in the design of these controllers. One design is similar to that used by (Pham et al. 1994) for the control of passenger vehicles. In the second SMC approach, the steering angle rate becomes the control command instead of the steering angle in the first approach. A feature common to the two SMC approaches is that an integrator can be naturally introduced into the feedback loop. In the first design, the presence of integral control assures static robust performance when the **signum** function, which appears in SMC, is replaced by a saturation function to eliminate chattering. The introduction of the integrator in the second SMC design is somewhat more natural. It filters the control chatter while retaining the asymptotic tracking ability. This controller was chosen for experimental study. At the time of writing this report an experimental bus was not available, therefore experiments were done on a passenger car, Pontiac 6000. For implementation of the controller, an adaptive robust lateral velocity observer was designed and implemented. Closed loop experiments conducted in Richmond Field Station included this observer. Although the focus of the present study is on SMC methodology, a discontinuous control technique, it is shown that a linear robust term is sufficient for asymptotic regulation. This design is also shown to be robust to singular perturbations caused by using filtered measurements.

# 1 Introduction

Lateral control of vehicles in Intelligent Vehicle Highway Systems (IVHS) and Automated Highway Systems (AHS) has been an active research subject in recent years. Much of the work in past has been concentrated in the area of light vehicles. Peng and Tomizuka (1993) applied Frequency Shaped Linear Quadratic (FSLQ) control to the problem of lateral (steering) control of the passenger car. Pham et al. (1994) applied Sliding Mode Control (SMC) to the problem of combined lateral and longitudinal control of passenger cars. Ackermann et al. (1995) applied SMC in a different manner from Pham et al. (1994) to the problem of lateral control of passenger cars. In this report lateral control of the commuter buses is considered. Commuter buses are roughly 10 times heavier than passenger vehicles. Hence the system response to a steering angle command is sluggish. Also there is greater likelihood of tire force saturation during cornering. The behavior of the vehicle is nonlinear at the saturation point of the tires (Peng 1992), (Bareket and Fancher 1989). Furthermore, bus parameters such as the mass and moments of inertia change often and over wide ranges and buses are more prone to roll over than passenger vehicles. Because of the above mentioned characteristics, robust or adaptive control is essential for the lateral control of commuter buses.

This report is a follow up of the Annual Report (Hingwe and Tomizuka 1995) submitted to PATH in 1995. Two SMC based controllers were studied from the perspective of lateral control of commuter buses. In this report, we present experimental evaluation of one of the controllers described in (Hingwe and Tomizuka 1995). For the sake of completeness, we summarize the design of the two SMCs. Only lateral and yaw dynamics of the buses are considered in the design of these controllers. One design is similar to that used by Pham et al. (1994) for the control of passenger vehicles. A linear combination of lateral error and yaw error, which in effect gives the lateral displacement of a point other than the center of gravity (CG) of the vehicle, is fed back to the controller. The combined error becomes input to the SMC. Another control approach presented here is motivated by Ackermann et al. (1995). We apply this control algorithm to the problem of lateral control of commuter buses with a different but equivalent formulation. The system is extended dynamically on the input side. Conventional SMC is then designed. A feature common between the two SMCs is

that an integrator gets naturally introduced into the feedback loop. In the first design, the integrator assures zero static error and in the second design, it filters the chattering due to the discontinuous robust term. Because the second design guarantees asymptotic tracking of the road centerline, it is chosen for experimental study.

Several implementation issues are presented and solved with respect to the above controller. A robust adaptive lateral observer, which is independent of the model parameters, is designed for lateral velocity estimation. Yaw-rate and yaw-angle are also estimated using stable filters. Two accelerometers were installed on the Pontiac 6000 for implementation of the SMC controller based on steering angle rate as the input. A passenger car had to be chosen for closed loop experimental study because at the time of writing this report, an experimental bus was unavailable. The success of the closed loop experiments has created confidence in the application of this methodology to commuter buses

Although the focus of this report is discontinuous control, it is of interest to note that because of the Lipschitz nature of the differential equations representing the car model, a continuous controller (instead of a discontinuous one) is sufficient to regulate the vehicle to the road center-line. Apart from parametric robustness, this controller is shown to be robust to singular perturbations arising from filtering of the states.

The remainder of this report is organized as follows. Section 2 contains the problem formulation along with the dynamic model of a commuter bus. The SMCs are designed in section 3. Section 4 discusses implementation issues and presents closed loop experiments. Conclusions are presented in section 5.

## **2 Lateral Control Problem for Commuter Buses**

In general the control objectives in lateral control of road vehicles for lane following are as follows:

1. Keeping lateral error at a selected point, e.g. at the center of gravity close to zero.

2. Maintaining the vehicle orientation parallel to the road orientation.

It is known that the orientation error, i.e. the yaw of the vehicle relative to the road orientation, cannot be made zero on a curve (at steady state) for vehicles which only have front wheel steering (Matsumoto and Tomizuka, 1992). Thus the control objective is to keep the lateral error of a certain point on the vehicle body zero while maintaining stability of the yaw dynamics.

## 2.1 The vehicle model

In this section, we describe the dynamic equations and the parameters of the vehicle model. The complex and simplified models of the passenger vehicle were derived by Peng (1992)

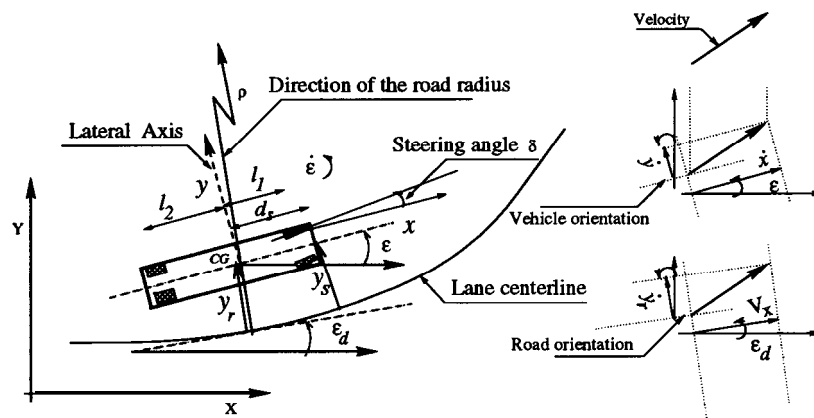


Figure 1: The description of the states, input and the output

and Patwardhan (1994). The vehicle model to be used for closed loop simulations for the commuter bus is essentially Peng's complex model (Peng 1992) with modification to accommodate weight shift due to roll and substitution of the tire model in Peng (1992) by a tire model suited to buses. Details of the tire model appropriate for commuter buses are given in Bareket and Fancher (1989). Open loop simulations show that the pitch dynamics are negligible. Roll dynamics, though not small, are not considered because the coupling between the roll and the steering input is rather weak. Thus, for the controller design, we consider



only the lateral and the yaw dynamics. The dynamic equations of the bus model for control design purpose are given by

$$\begin{aligned}
m\ddot{y} &= -m\dot{\epsilon}\dot{x} - 2C_{\alpha_r}(\dot{y} - \dot{\epsilon}l_2)/\dot{x} \\
&\quad - 2C_{\alpha_f}(\dot{y} + \dot{\epsilon}l_1)/\dot{x} + 2C_{\alpha_f}\delta \\
\ddot{y} &\triangleq f_1(\mathbf{x}) + b_1\delta \\
I_z\ddot{\epsilon} &= 2l_2C_{\alpha_r}(\dot{y} - \dot{\epsilon}l_2)/\dot{x} - 2l_1C_{\alpha_f}(\dot{y} + \dot{\epsilon}l_1)/\dot{x} \\
&\quad + 2l_1C_{\alpha_f}\delta \\
\ddot{\epsilon} &\triangleq f_2(\mathbf{x}) + b_2\delta
\end{aligned} \tag{1}$$

where,

$\dot{y}$  = Vehicle velocity along the lateral principle axis of the sprung mass of the vehicle in **m/s**,

$\ddot{y}$  = Vehicle linear acceleration in the lateral principle direction in  $m/s^2$ ,

$\dot{\epsilon}$  = Yaw rate of the vehicle in  $rad/s$  (refer Figure 1),

$\ddot{\epsilon}$  = Angular acceleration of the vehicle in the yaw direction in  $rad/s^2$ ,

$\dot{x}$  = Longitudinal velocity of the vehicle (component along the road) in **m/s**,

$m$  = Mass of the vehicle in **kg** (10,000 – 16,000),

$I_z$  = Yaw moment of inertia in  $kgm^2$  (171,050),

$l_1$  = Longitudinal distance of the front axle from the center of gravity in **m** (3.67),

$l_2$  = Longitudinal distance of the rear axle from the center of gravity in **m** (1.93),

$C_{\alpha_r}$  = Cornering stiffness of the rear tires in  $KN/rad$  (425),

$C_{\alpha_f}$  = Cornering stiffness of the front tires in  $KN/rad$  (213),

$\delta$  = steering angle (input) in **rad**,

$f_1(\mathbf{x}) \triangleq (-m\dot{\epsilon}\dot{x} - K_{wy}\dot{y}|\dot{y}| - 2C_{\alpha_r}(\dot{y} - \dot{\epsilon}l_2)/\dot{x}$

$- 2C_{\alpha_f}(\dot{y} + \dot{\epsilon}l_1)/\dot{x})/m$ ,

$\mathbf{x}$  is the state vector comprising of  $[y, \dot{y}, \epsilon, \dot{\epsilon}]$ ,

$b_1 \triangleq 2C_{\alpha_f}/m$ ,

$f_2(\mathbf{x}) \triangleq (2l_2C_{\alpha_r}(\dot{y} - \dot{\epsilon}l_2)/\dot{x} - 2l_1C_{\alpha_f}(\dot{y} + \dot{\epsilon}l_1)/\dot{x})/I_z$  and

$b_2 \triangleq (2l_1C_{\alpha_f})/I_z$ .

The values in parentheses are nominal or range of corresponding parameter. Because we are interested in keeping the lateral error of a certain point on the vehicle zero, we define the lateral error at this point as  $y_s$ . This point is located a distance  $d_s$  ahead of the center

of gravity (CG) of the vehicle and is shown in Figure 1. A lateral error sensor is located at this point.  $y_s$  is given by

$$y_s = y_r + d_s(\epsilon - \epsilon_d) \quad (2)$$

where  $y_r$  is the lateral position of the CG of the vehicle with respect to the road centerline,  $\epsilon_d$  is the yaw angle of the road with respect to a global coordinate system (see Figure 1) and  $\epsilon$  is the yaw angle of the vehicle with respect to the same global coordinate system as in the definition of  $\epsilon_d$ . Road yaw rate, given by  $\dot{\epsilon}_d = V_x/R$  where  $R$  is the road radius, is assumed available.  $V_x$  is the longitudinal velocity of the vehicle along the road.

For the control design, we will require that  $\ddot{\epsilon}_d$  be piecewise continuous. This can be achieved by filtering the road curvature data. Since the quantity of interest for control purposes is  $y_s$ , it is judicious to write down the state equations in terms of the output  $y_s$  that we want to regulate. The transformation from body fixed coordinates to the road coordinates gives us the following dynamical equations representing the plant model.

$$\begin{aligned} \frac{d}{dt}y_s &= \dot{y}_s \\ \frac{d}{dt}\dot{y}_s &= (\ddot{y} + d_s\ddot{\epsilon})\cos(\epsilon - \epsilon_d) + (\ddot{x} - d_s\epsilon^2)\sin(\epsilon - \epsilon_d) - V_x^2/R \end{aligned}$$

With the help of equation (1), the above equations can be rewritten as

$$\begin{aligned} \frac{d}{dt}y_s &= \dot{y}_s \\ \frac{d}{dt}\dot{y}_s &= -\dot{\epsilon}\dot{x} - 2C_{\alpha_r}/m(\dot{y} - \dot{\epsilon}l_2)/\dot{x} - 2C_{\alpha_f}/m(\dot{y} + \dot{\epsilon}l_1)/\dot{x} \\ &\quad + 2C_{\alpha_f}/m\delta + 2d_sl_2C_{\alpha_r}/I_z(\dot{y} - \dot{\epsilon}l_2)/\dot{x} \\ &\quad - 2d_sl_1C_{\alpha_f}/I_z(\dot{y} + \dot{\epsilon}l_1)/\dot{x} + 2d_sl_1C_{\alpha_f}/I_z\delta + (\ddot{x} - d_s\epsilon^2)(\epsilon - \epsilon_d) - V_x^2/R \\ &\triangleq f(x) + b\delta \end{aligned} \quad (3)$$

where

$$\begin{aligned} f(x) &= -\dot{\epsilon}\dot{x} - 2C_{\alpha_r}/m(\dot{y} - \dot{\epsilon}l_2)/\dot{x} - 2C_{\alpha_f}/m(\dot{y} + \dot{\epsilon}l_1)/\dot{x} + 2d_sl_2C_{\alpha_r}/I_z(\dot{y} - \dot{\epsilon}l_2)/\dot{x} \\ &\quad - 2d_sl_1C_{\alpha_f}/I_z(\dot{y} + \dot{\epsilon}l_1)/\dot{x} + (\ddot{x} - d_s\epsilon^2)(\epsilon - \epsilon_d) - V_x^2/R \end{aligned}$$

and  $b = 2C_{\alpha_f}/(1/m + d_sl_1/I_z)$

The input to the plant is  $\delta$  and the output is  $y_s$ . The controller designs summarized in the following section will utilize the above equations.

### 3 Controller Design

In this section, we present two SMC based controllers for lateral control of buses. As stated earlier, one control objective is to keep the bus lateral error zero and yaw error bounded at all times. Ride comfort has to be maintained. Additionally, steering angle is limited to approximately 0.5 **rad** and the steering angle rate to 0.5rad/s. The assumptions for the controller design are :

- All states are available,
- $f_2(\mathbf{x})$  is sufficiently smooth and
- road yaw rate,  $\dot{\epsilon}_d$ , which will occur in the controller design, is sufficiently smooth.

#### 3.1 Sliding Mode Controller Design - I

In this section we present the design of a Sliding Mode Controller for lateral control of commuter buses. The formulation of the control law follows from Pham et al. (1994). Essentially, the SMC methodology consists of defining a sliding surface variable  $s$ , given by

$$s \triangleq \dot{e} + \lambda e, \quad \lambda > 0. \quad (4)$$

where  $e$ , the tracking error, is the difference in the actual lateral error at the sensor  $y_s$  and the desired lateral error at the sensor  $y_{s_d}$ . If we devise a control law such that

$$s\dot{s} \leq -\eta|s|, \quad \eta > 0, \quad (5)$$

then we are assured of reaching the sliding surface ( $s = 0$ ) within a finite time, given by  $s(t_0)/\eta$ , where  $t_0$  is the initial time. Once on this surface, the system stays on it. The functions  $f(x)$  and  $\mathbf{b}$  (equation 3) are not known exactly but their nominal values are known in terms of the nominal values of plant parameters and current state. Let these be denoted by  $\hat{f}(\mathbf{x})$  and  $\hat{\mathbf{b}}$ . Our task is to construct, given the bounds on  $f(x)$  and  $\mathbf{b}$ , a control law such that the system is driven to the sliding surface in the way prescribed by inequality (5). It is assumed that  $f(x)$  and  $\mathbf{b}$  satisfy the following inequalities:

$$|f - \hat{f}| \leq F \quad \text{and} \quad b_{min} \leq b \leq b_{max} \quad (6)$$

where  $F$ ,  $b_{max}$  and  $b_{min}$  are known. It can be verified that the control law

$$\delta = (\mathbf{ii} - \mathbf{k} \operatorname{sgn}(s)) / \hat{b} \quad (7)$$

ensures the satisfaction of inequality (5).

In equation (7),  $k \geq \beta(F + \eta) + (\beta - 1)|\hat{u}|$ ,  $\beta = (b_{max}/b_{min})^{1/2}$ ,  $\hat{u} = -\hat{f} + (\ddot{y}_{s_d}) - \lambda(\dot{y}_s - \dot{y}_{s_d})$ ,  $\dot{y}_{s_d}$  and  $\ddot{y}_{s_d}$  are the desired lateral velocity and the desired lateral acceleration at the sensor location respectively. Note that in our application  $\dot{y}_{s_d}$  and  $\ddot{y}_{s_d}$  are identically zero. Control law given by equation (7) ensures that sliding at  $s = 0$  is guaranteed to take place. Since the error dynamics (equation 4) is asymptotically stable for  $s = 0$ , the control law (equation 7) assures that the lateral error  $y_s$  will go to zero.

However, because of the presence of  $\mathbf{k} \operatorname{sgn}(s)$  in the control law, the input  $\delta$  to the plant chatters. This may be detrimental to the steering actuator. One way to smooth the control is to use  $\operatorname{sat}(s/\Phi)$ , a saturation function, in place of  $\operatorname{sgn}(s)$  in the control law.  $\Phi$  is the boundary layer thickness around the sliding surface  $s = 0$  where the saturation function is linear in  $s/\Phi$ . In this case it is not assured that  $s$  goes to zero. A partial solution to this problem is to redefine the sliding variable  $s$  as

$$\begin{aligned} s &= \dot{e} + (\lambda_1 + \lambda_2)e + \lambda_1 \lambda_2 \int_{t_0}^t \mathbf{e}(\boldsymbol{\tau}) d\boldsymbol{\tau} \\ &= (D + \lambda_1)(D + \lambda_2)v(t) \end{aligned} \quad (8)$$

where

$$\mathbf{v}(t) = \int_0^t \mathbf{e}(\boldsymbol{\tau}) d\boldsymbol{\tau}. \quad (9)$$

$\mathbf{v}(t)$  can be considered the output of the augmented plant (see Figure 2). The control law is modified to

$$\delta = 1/\hat{b}(\hat{u} - k \operatorname{sat}(s/\Phi))$$

where  $s$  is given by equation (8) and  $\hat{u}$  is given by

$$\hat{u} = -\hat{f} + (\ddot{y}_{s_d}) - (\lambda_1 + \lambda_2)\dot{e} - \lambda_1 \lambda_2 e \quad (10)$$

The gain  $\mathbf{k}$  remains as defined in equation (6). Though the above control law does not imply convergence of tracking error,  $e$ , the tracking error will be close to zero when the combined

effect of the disturbances and uncertainties is nearly constant in the region  $|s| < \Phi$ . The closed loop system is summarized in Figure 2. Note the presence of an integrator in the path from  $y_s$  to  $\delta$ . In the next section, we design a SMC with steering rate as the input to the

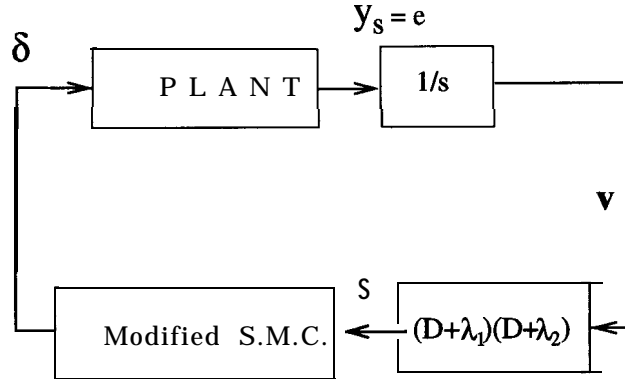


Figure 2: Block diagram of controller one

vehicle.

### 3.2 Sliding Mode Controller Design II

This section describes a different approach to the SMC design for lateral control of buses. This approach is motivated by Ackermann et al. (1995) in which the lateral control problem is tackled in two stages. First, a desired yaw rate which stabilizes the lateral dynamics at the sensor is computed. Then a controller which uses conventional SMC methodology is designed to track the desired yaw rate. We had shown in (Hingwe and Tomizuka 1995) that there was an equivalent way of designing this controller. The main benefit of the alternative perspective was that asymptotic stability could be shown. In the remaining section, we summarize the control design.

Consider a dynamic extension of the system as given below

$$\begin{aligned}
 \frac{d}{dt}y_s &= \dot{y}_s \\
 \frac{d}{dt}\dot{y}_s &= \ddot{y}_s \\
 \frac{d}{dt}\ddot{y}_s &= f^* + b\delta^*
 \end{aligned} \tag{11}$$

where  $f^* = f$  and  $\delta^* = \delta$ . We assume that we do not know the value of system parameters in  $f^*$  and  $b$  exactly. Let  $\hat{f}^*$  and  $\hat{b}$  be the nominal representation of  $f^*$  and  $b$  respectively in terms of the nominal parameter values and system state.  $f^*$ ,  $\hat{f}^*$  and  $\mathbf{b}$  satisfy

$$b_{min} \leq b \leq b_{max} \quad |\hat{f}^* - f^*| \leq \mathbf{F}^*$$

where  $\mathbf{F}^*$ ,  $b_{min}$  and  $b_{max}$  are known. We define the sliding surface variable  $s$  as

$$s = (D + \lambda)(D + k)y_s \quad (12)$$

where  $\lambda$  and  $\mathbf{k}$  are positive and construct a control law  $\delta^*$  given by

$$\delta^* = (\hat{u} - \mathbf{K} \operatorname{sgn}(s)) / \hat{b} \quad (13)$$

where

$$\begin{aligned} \hat{u} &= -\hat{f}^* - (\mathbf{k} + \lambda)\ddot{y}_s - k\lambda\dot{y}_s, \\ \mathbf{k} &\geq \beta(\mathbf{F}^* + \eta) + (\beta - 1)|\hat{u}|, \end{aligned}$$

and

$$\beta = (b_{max}/b_{min})^{1/2}.$$

It can be easily checked that  $s\dot{s} \leq -\eta|s|$ . If  $\eta > 0$ , we are assured that  $s$  goes to zero in finite time. Sliding takes place after  $s = 0$  and  $y_s$  goes to zero asymptotically. The algorithm is summarized in Figure 3. We can see that this algorithm introduces an integrator in the feedback loop. The integrator appears ahead of the plant. This integrator filters off chatter in  $\delta^*$ .

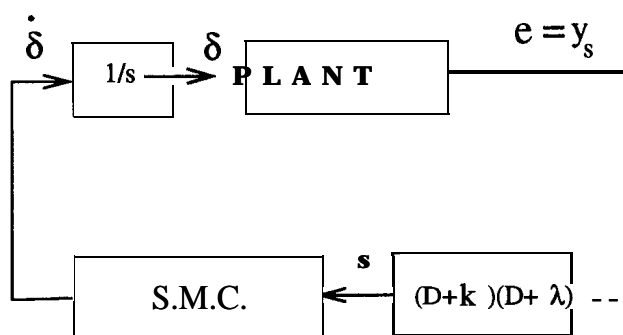


Figure 3: Block Diagram of the second controller seen as input filtering

By comparing Figure (2) and Figure (3), it can be seen that the difference between Design I and Design II is in the placement of the free integrator. Design II eliminates chatter while

preserving asymptotic tracking. Because of this, Design II was chosen for implementation and experimental study.

## 4 Experimental Evaluation of Design II

Experimental evaluation of the SMC using steering rate as an input was done on the Pontiac 6000, the PATH research car. Because a bicycle model was used in the control design, the controller design is valid for passenger cars. This section is divided into two parts. The first part discusses the measurements needed to implement the controller. Sensors used to get these measurements and observers used to estimate the non-measurable states are discussed. The second part gives a description of the experimental set up and presents some closed loop experimental results from Richmond Field Station test-track.

### 4.1 Measuring and estimation of the states

The SMC methodology is based on feedback linearization and requires the following quantities as feedback information.

- output  $y_s$
- Lateral Velocity  $\dot{y}$
- Yaw-angle  $\epsilon - \epsilon_d$
- Yaw-rate  $\dot{\epsilon}$
- Desired Yaw-rate  $\dot{\epsilon}_d$
- Lateral acceleration  $\ddot{y}$
- Yaw-acceleration  $\ddot{\epsilon}$
- Desired Yaw-acceleration  $\ddot{\epsilon}_d$

At present, most of these quantities are directly measured. A list of the relevant sensors on the Pontiac 6000 is given below:

- Magnetometers at the front and the rear end of the vehicle. These give lateral distance from the magnets (embedded along the road centerline).
- Yaw-rate sensor.
- Lateral accelerometers at
  - center of gravity
  - Front end of the vehicle
  - Rear end of the vehicle

The accelerometers at the front and the rear ends were installed in the course of the present project. The sensors were mounted on aluminum brackets which in turn were mounted on the car body. The sensors were calibrated against the accelerometer at the CG.

The sensors mentioned above can be used to obtain all the state measurement except lateral velocity. We propose the following robust observer for lateral velocity estimation.

### **Lateral velocity observer**

From kinematics, we have the following equation

$$\begin{aligned} \frac{d}{dt} y_s &= \dot{y} + \dot{x}(\tilde{\epsilon}) + d_s * (\dot{\epsilon} - \mathbf{id}) \\ \frac{d}{dt} \dot{y} &= \ddot{y} \end{aligned} \tag{14}$$

where  $\tilde{\epsilon} = \epsilon - \epsilon_d$ .



Based on the above equation and the assumption that acceleration along the body lateral axis can be measured, we propose the following observer.

$$\begin{aligned}\frac{d}{dt} \hat{y}_s &= \hat{y} + \dot{x}(\tilde{\epsilon}) + d_s * (\dot{\epsilon} - \dot{\epsilon}_d) \\ &\quad + k_1(y_s - \hat{y}_s) \\ \frac{d}{dt} \hat{y} &= \ddot{y} - V_x^2/R + k_2(y_s - \hat{y}_s)\end{aligned}\tag{15}$$

where,  $\hat{y}_s$  is the estimate of the lateral error at the front bumper and  $\hat{y}$  is the estimate of the lateral velocity. Assuming that we can measure yaw rate ( $\dot{\epsilon}$ ), longitudinal velocities ( $\dot{x}$  and  $V_x$ ) and have the knowledge of road radius of curvature ( $R$ ) and distance of lateral error sensor from CG ( $d_s$ ), the following equations can be deduced from equations (14) and (15).

$$\frac{d}{dt} \begin{bmatrix} y_s - \hat{y}_s \\ \dot{y} - \hat{y} \end{bmatrix} = \begin{bmatrix} -k_1 & 1 \\ -k_2 & 0 \end{bmatrix} \begin{bmatrix} y_s - \hat{y}_s \\ \dot{y} - \hat{y} \end{bmatrix}\tag{16}$$

The characteristic equation of the above system is  $s^2 + k_1s + k_2$ . The poles of the observer can be placed by appropriately choosing  $k_1$  and  $k_2$ . Note that this observer is in the form of a Kalman Filter and hence can be made optimal if the noise covariances of the measurements are known. It can be seen that apart from the knowledge of  $d_s$ , the observer is independent of the plant model and is hence kinematic.

The dependence of observer on the term  $d_s$  can be taken care of by adapting the value of  $d_s$ . The following simple adaptive scheme is proposed. Consider a Lyapunov function candidate  $V$  given by

$$2V = \begin{bmatrix} y_s - \hat{y}_s & \dot{y} - \hat{y} \end{bmatrix} P \begin{bmatrix} y_s - \hat{y}_s \\ \dot{y} - \hat{y} \end{bmatrix} + \gamma(d_s - \hat{d}_s)^2\tag{17}$$

where  $P$  is the solution of the Lyapunov equation

$$PA + A^T P = -I$$

and  $\hat{d}_s$  is the estimate of  $d_s$ . The derivative of the Lyapunov Function candidate along the trajectories of the system (15) is given by

$$\dot{V} = - \begin{bmatrix} y_s - \hat{y}_s & \dot{y} - \hat{y} \end{bmatrix} I \begin{bmatrix} y_s - \hat{y}_s \\ \dot{y} - \hat{y} \end{bmatrix} + (d_s - \hat{d}_s)(\dot{\epsilon}_d - \dot{\epsilon} + \gamma\dot{\hat{d}}_s)\tag{18}$$

By letting

$$\dot{\hat{d}}_s = \frac{1}{\gamma}(\dot{\epsilon} - \epsilon_d) \quad (19)$$

$\dot{V}$  given by equation (18) becomes negative semidefinite. From La Salle's invariant set theorem (Slotine 1991), we can conclude that the estimation error  $\begin{bmatrix} y_s - \hat{y}_s & \dot{y} - \hat{\dot{y}} \end{bmatrix}$  converges to zero asymptotically. However, the parameter  $\hat{d}_s$  may not necessarily converge to  $d_s$ . Having taken care of the measurement and estimation of state variables, we examine some implementation problems associated with measurements.

It can be seen from Figure 3 that the implementation of the controller requires the measurement of acceleration. There are two practical problems associated with the acceleration feedback. Firstly, the lateral acceleration signal for low speeds and large radii of curvature of the road is very small. Therefore the noise to signal ratio is high. Secondly, because the accelerometers have to be mounted on the sprung mass of the passenger cars - a problem which will not exist in the case of heavy vehicles such as commuter buses - the component of acceleration due to gravity in the direction of vehicle roll is contained in the sensor output. Note that the acceleration signal is used in two places in the control law: 1. For canceling the nonlinearities (given as  $-f^*$ ) and 2., for evaluating the sliding surface variable term in  $Ksign(s)$ . The nonlinear functions are very sensitive to noise in their arguments. We take care of this problem by analytically integrating part of the control law and by filtering where necessary.

Recall that the control law given by equation (13) is

$$\dot{\delta} = 1/\hat{b}(-\hat{f}^* - (\lambda + k)\ddot{y}_s - \lambda k\dot{y}_s - Ksign(s))$$

Therefore,

$$\begin{aligned} \delta &= \int_{t_0}^t 1/\hat{b}(-\hat{f}^* - (\lambda + k)\ddot{y}_s - \lambda k\dot{y}_s - Ksign(s)) d\tau \\ \delta &= 1/\hat{b}\left(-\hat{f} - (\lambda + k)\dot{y}_s - \lambda ky_s - \int_{t_0}^t Ksign(s)d\tau\right) \end{aligned}$$

Notice that the control law now requires the acceleration measurement only for computing  $s$ .  $\int_{t_0}^t Ksign(s)d\tau$  cannot be analytically integrated and hence the filtering of variable  $s$  becomes necessary.

The control law now becomes,

$$\delta = 1/\hat{b} \left( -\hat{f} - \alpha_1 \dot{y}_s - \alpha_2 y_s - \int_{t_0}^t K \text{sign}(\nu) d\tau \right)$$

$$\tau \dot{\nu} + \nu = s$$

where  $\alpha_1 = (k + \lambda)$  and  $\alpha_2 = k\lambda$  with  $\mathbf{k}$  and  $\lambda$  as defined in equation (12). The implementation of this control is summarized in Figure (4). Experimental results presented in section 4 are based on this control law.

Although the focus of this report is SMCs, it is of interest to note that the discontinuous robust term ( $\text{sign}(s)$ ), is not required to achieve regulation of the system to  $y_s = 0$ . A sufficient condition for regulation of the system under consideration is that the control law be

$$\delta^* = 1/\hat{b} (-f^* - \alpha_1 \ddot{y}_s - \alpha_2 \dot{y}_s - K\nu)$$

where

$$\tau \dot{\nu} + \nu = s$$

and  $\mathbf{K}$  and  $\tau$  are design parameters. The proof of this claim is given in Appendix B.

## 4.2 Closed loop Experiments

Closed loop experiments for Design II were performed in the Richmond Field Station. The test track is shown in Figure 5. The experimental setup in the Pontiac 6000 is adequately described in Peng (1992) and Hessburg (1994). The same hardware and software was used to implement the SMC. The closed loop experiments are summarized in Figures 6, 7 and 8. The Lateral-error plots show the distance from the magnetic markers on the test track to the front magnetometer (bold line) and the rear magnetometer (dashed line).

The tracking error is comparable to the tracking error obtained by previous researchers using Frequency Shaped Linear Quadratic (FSLQ) (Peng et al. 1992) and marginally better than (Fuzzy Logic Control) (Hessburg et al. 1994). The peak tracking error was typically within  $\pm 10$  **cm**. Tracking error can be made smaller by making the sliding mode dynamics faster, but passenger comfort is compromised. An important advantage of the SMC as

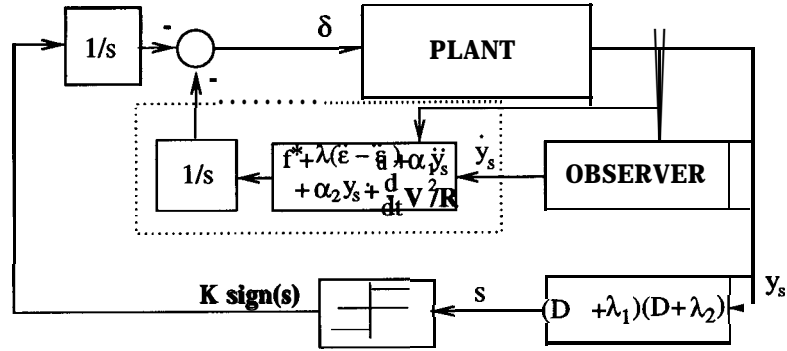


Figure 4: Implementation of Controller II

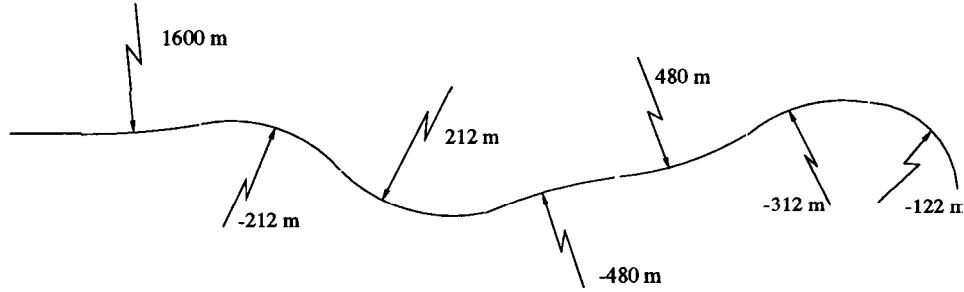


Figure 5: Richmond Field Station Track

seen from the longitudinal velocity plots in Figures (6) - (7) is that the tracking error is insensitive to variation in longitudinal velocity. Unlike linear algorithms (e.g. FSLQ), no gain scheduling is necessary.

Apart from passenger comfort, there are other limitations to the design of sliding surface. Due to the noise in measurements used for the lateral velocity observer, the observer cannot be made very vast. This limits how fast the sliding mode dynamics can be designed. A steering actuator with bandwidth of about 3-4 Hz is another factor in limiting the design of the sliding mode dynamics.

The control design does not account for the internal dynamics in yaw. The internal dynamics are not observable from the output  $y_s$ , but they are felt by the passengers as uncomfortable oscillations. Although the internal dynamics in the present case is stable, quickly changing road radius at the Richmond Field Station keeps them sustained. Some correlation was found between these yaw oscillations and the sliding surface parameters  $\alpha_1$  and  $\alpha_2$ . It was seen that the slower sliding surface dynamics reduced the oscillations significantly.

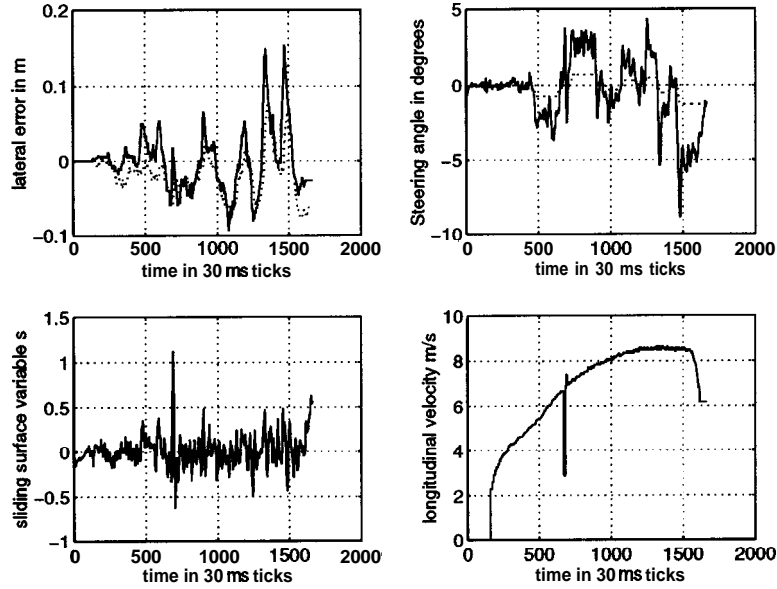


Figure 6: Experiments with  $\alpha_1 = 6$  and  $\alpha_2 = 8$

Another possible reason for the oscillations may be the oscillation of the steering angle as seen in Figures (6) - (7). This oscillation may occur because of the high gain robust term  $\int_{t_0}^t K \text{sign}(\nu) d\tau$  term. From the plots of sliding surface variable  $s$  v/s time in Figures (6) - (7), it can be seen that  $\int_{t_0}^t K \text{sign}(\nu) d\tau$  may be oscillatory. The remedy to this problem lies in transferring some burden of robustness from the high gain term to adaptation.

Another strategy to make the yaw dynamics benign may be output redefinition. Because the yaw dynamics have a pole at  $-\frac{V_x}{d_s}$  (Hingwe and Tomizuka 1995), projecting the lateral sensor measurement to a point ahead of the vehicle (which will increase  $d_s$ ) should decrease oscillations.

## 5 Conclusions

Two SMC based controllers were applied to the problem of lateral control of commuter buses. The reduction of the chatter, which appears in the control action due to the presence of the **sign** function in SMC design, was one of the objectives. A boundary layer was added to smooth the control in the first approach. However, we lose the robust asymptotic tracking of the Sliding Mode Control design methodology. In the second controller, an integrator

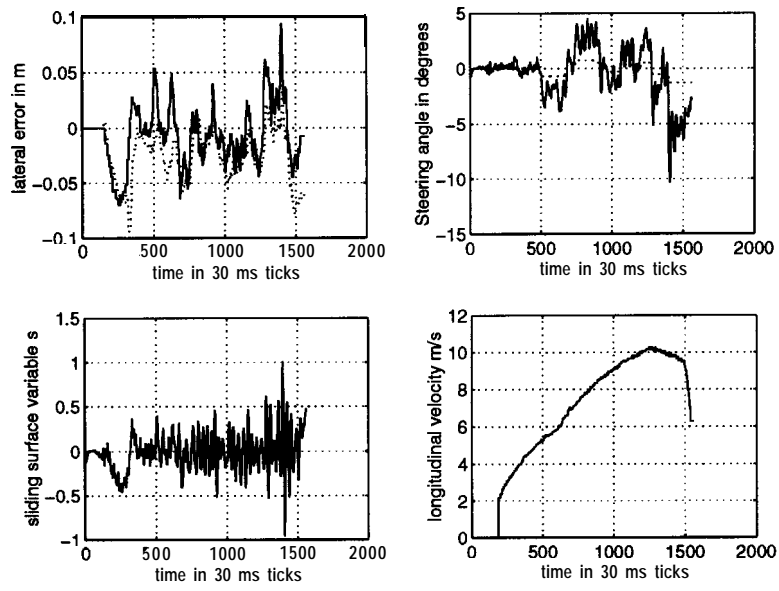


Figure 7: Experiments with  $\alpha_1 = 6$  and  $\alpha_2 = 10$

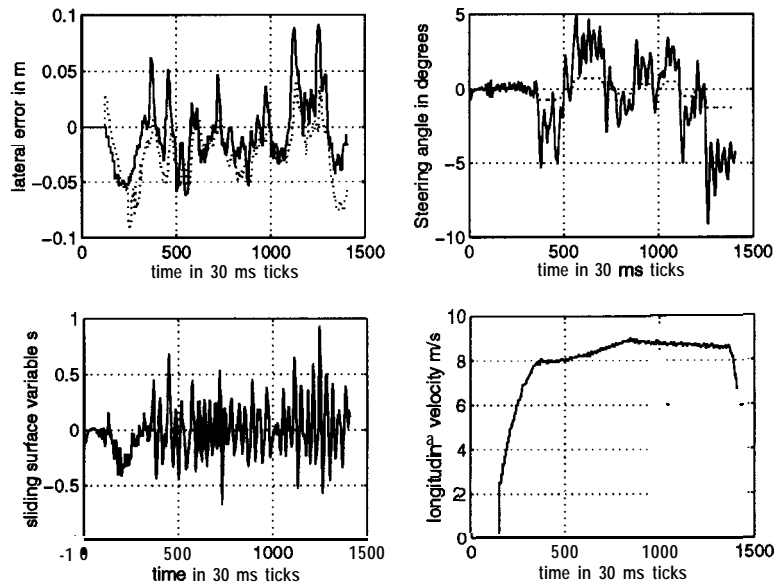


Figure 8: Experiments with  $\alpha_1 = 6$  and  $\alpha_2 = 10$

naturally appeared in the feedback loop, but at the input of the plant. This eliminated the chatter in the input to the plant. The ideal sliding mode was maintained. Hence asymptotic error convergence to zero is guaranteed. The experimental results show the validity of the model and of the control design strategy based on the steering rate control. Experimental results show that tracking error comparable to the linear controllers can be achieved by using a theoretically sound robust nonlinear control.

**Acknowledgement** We wish to thank Dr. D. Swaroop for his help with the proof of stability presented in Appendix B. We also wish to thank Daimler Benz, Germany, for providing the nominal parameters of a commuter bus.

## References

- [1] Ackermann, J., Guldner, J., Sienel, W., Steinhauser, R., 1995 "Linear and Nonlinear Controller Design for Robust Automatic Steering," *IEEE Trans. on Control Systems Technology*, Vol 3, pp. 132-143.
- [2] Bareket Z., Fancher P., 1989, "Representation of Truck Tire Properties in Braking and Handling Studies, Influence of Pavement and Tire Conditions on the Friction Characteristics," Technical Report UMTRI-8933, Univ. of Michigan, Ann Arbour, MI.
- [3] Hingwe, P. and Tomizuka M., 1995, "Lateral Control of Commuter Buses", PATH Working Paper, ITS, UC Berkeley, no. UCB-ITS-PWP-95-9.
- [4] Khalil, H. K., *Nonlinear Systems*, Macmillan Publishing Company, 1992.
- [5] Patwardhan, S., 1994 "Fault Detection and Tolerant Control for Lateral Guidance of Vehicles in Automated Highways," PhD thesis, UC Berkeley, CA.
- [6] Peng, H., 1992, "Vehicle Lateral Control for Highway Automation," PhD Thesis, UC Berkeley, CA.
- [7] Peng, H. and Tomizuka, M., 1993, "Preview Control for Vehicle Lateral Guidance in Highway Automation," *ASME Journal of Dynamic Systems, Measurement and Control*, Vol. 115, No. 4, pp. 678-686.

- [8] Peng, H., Zhang, W., Arai, A., Lin, Y., Hessburg, T., Develin, P., Tomizuka, M. and Shladover, S., 1992, "Experimental Automatic Lateral Control System for an Automobile", PATH Research Report, ITS, UC Berkeley, no. UCB-ITS-PRR-92-11.
- [9] Pham, H., Hedrick, K. and Tomizuka, M., 1994, "Combined Lateral and Longitudinal Control of Vehicles," ***Proceedings of the American Control Conference***, Baltimore, Maryland, pp. 1205-1206.
- [10] Matsumoto, N. and Tomizuka, M., 1992, "Vehicle Lateral Velocity and Yaw Rate Control with Two Independent Inputs," ***ASME Journal of Dynamic Systems, Measurement and Control***, Vol 114, pp. 606-612.
- [11] Slotine, J. and Li, W., ***Applied Nonlinear Control***, Prentice Hall, 1991.
- [12] Hessburg, T., Peng, H., Zhang, W., Arai, A., Tomizuka, M., 1994, "Experimental Results of Fuzzy Logic Control for Lateral Vehicle Guidance", California PATH research paper, ITS, UC Berkeley, no. UCB-ITS-PRR-94-03.
- [13] Tsao, H-S. J., 1995, "Constraints on Initial AHS Deployment and the Concept Definition of a Shuttle Service for AHS Debut", ***IVHS Journal***, Vol. 2(2), pp. 159-173.



## APPENDIX A. Parameters for experimental car (Pontiac 6000)

Nominal values

- mass = 1485 kg
- $I_z = 2782kg/m^2$
- $C_{\alpha r} = 42000N/rad$
- $C_{\alpha f} = 42000N/rad$
- $l_1 = 1.1m$
- $l_2 = 1.58m$
- $d_s = 1.96m$

Parameter ranges

- min mass = 1300 kg , max mass = 1600 kg
- min  $I_z = 1400kg/m^2$  , max  $I_z = 3000kg/m^2$
- min  $C_{\alpha r} = 38000N/rad$ , max  $C_{\alpha r} = 42000N/rad$
- min  $C_{\alpha f} = 38000N/rad$ , max  $C_{\alpha f} = 42000N/rad$
- $\eta = .25$

Parameter values used in the observer

- $k_1 = 15$ ,  $k_2 = \mathbf{50}$
- $\hat{d}_s(t = \mathbf{0}) = \mathbf{2m}$

## APPENDIX B. Continuous robust control design

Consider the model of the vehicle described by equations (11), which restated is

$$\begin{aligned}\frac{d}{dt}y_s &= \dot{y}_s \\ \frac{d}{dt}\dot{y}_s &= \ddot{y}_s \\ \frac{d}{dt}\ddot{y}_s &= f^* + b\delta\end{aligned}$$

recall from equation (3)

$$\frac{d}{dt}\ddot{y}_s = -\dot{\epsilon} - V_x^2/R + (\ddot{x} - d_s\dot{\epsilon}^2)(\epsilon - \epsilon_d)$$

$$\begin{aligned}+ \frac{-2}{\dot{x}} \begin{bmatrix} C_{\alpha_f}(\frac{1}{m} + \frac{l_1 d_s}{I_z}) + C_{\alpha_r}(\frac{1}{m} - \frac{l_2 d_s}{I_z}) \\ C_{\alpha_f}(\frac{1}{m} + \frac{l_1^2 d_s}{I_z}) + C_{\alpha_r}(\frac{1}{m} - \frac{l_1^2 d_s}{I_z}) \end{bmatrix}^T \begin{bmatrix} \dot{y} \\ \dot{\epsilon} \end{bmatrix} \\ + 2C_{\alpha_f}(1/m + l_1 d_s/I_z)\delta\end{aligned}\quad (20)$$

$$\triangleq g + \Theta^T \frac{1}{\dot{x}} \begin{bmatrix} \dot{y} \\ \dot{\epsilon} \end{bmatrix} + b\delta\quad (21)$$

where  $g = -\dot{\epsilon} - V_x^2/R + (\ddot{x} - d_s\dot{\epsilon}^2)(\epsilon - \epsilon_d)$  and

$$\Theta^T = -2 \begin{bmatrix} C_{\alpha_f}(\frac{1}{m} + \frac{l_1 d_s}{I_z}) + C_{\alpha_r}(\frac{1}{m} - \frac{l_2 d_s}{I_z}) \\ C_{\alpha_f}(\frac{1}{m} + \frac{l_1^2 d_s}{I_z}) + C_{\alpha_r}(\frac{1}{m} - \frac{l_1^2 d_s}{I_z}) \end{bmatrix}^T$$

Notice that  $1/\dot{x}$  can be treated as a known parameter and it is trivial to see that  $\begin{bmatrix} \dot{y} \\ \dot{\epsilon} \end{bmatrix} \mathbf{1}$  is Lipschitz. Dynamically extending the system, we obtain the following representation

$$\frac{d}{dt}\ddot{y}_s = \dot{g} + \begin{bmatrix} \Theta^T & \Theta^T \\ \frac{\Theta^T}{\ddot{x}} & \frac{\Theta^T}{\dot{x}} \end{bmatrix} \begin{bmatrix} \dot{y} \\ \dot{\epsilon} \\ \ddot{y} \\ \ddot{\epsilon} \end{bmatrix} + b\dot{\delta}\quad (22)$$

If  $\ddot{x}$  and  $\dot{x}$  are treated as measured parameters, then  $[\dot{y} \dot{\epsilon} \ddot{y} \ddot{\epsilon}]^T$  is Lipschitz. For notational simplicity, we rewrite the system as

$$\begin{aligned}\frac{d}{dt}x_1 &= x_2 \\ \frac{d}{dt}x_2 &= x_3 \\ \frac{d}{dt}x_3 &= \dot{g} + \Theta^T f + u\end{aligned}\quad (23)$$

where, by abuse of notation,  $\Theta^T = \begin{bmatrix} \Theta^T & \Theta^T \\ \frac{\Theta^T}{\ddot{x}} & \frac{\Theta^T}{\dot{x}} \end{bmatrix}$ . It can be verified that the control law given by

$$u = -\dot{g} - Of - \alpha_1 x_3 - \alpha_2 x_2 - Ks$$

where

$$s = x_3 + \alpha_1 x_2 + \alpha_2 x_1$$

results in  $\dot{s} = -Ks$ . Because  $s$  goes to zero asymptotically and  $s = 0$  is a stable system (by design of  $\alpha_1$  and  $\alpha_2$ ),  $x_1$  converges to zero. Note that the  $x_3$  is an acceleration term. A low pass filter is used to smooth the acceleration measurement. Also, parameter vector  $\Theta$  is unknown. A nominal value  $\hat{\Theta}$  is used. Bound on  $\Theta$  is assumed to be known. Under these assumptions the control law is,

$$\mathbf{u} = -\dot{g} - \hat{\Theta}f - \alpha_1 x_3 - \alpha_2 x_2 - \mathbf{K}\mathbf{u} \quad (24)$$

$$\tau\dot{\nu} + \nu = s \quad (25)$$

If the filter is fast enough, then the asymptotic regulation is maintained. In presence of the singular perturbation given by equation (25), the feedback system consists of two natural parts. One part is called the reduced system and is given by

$$\begin{aligned} \frac{d}{dt} x_1 &= x_2 \\ \frac{d}{dt} x_2 &= x_3 \\ \frac{d}{dt} x_3 &= (\Theta - \hat{\Theta}) - \alpha_1 x_3 - \alpha_2 x_2 - \mathbf{K} \mathbf{u} \end{aligned} \quad (26)$$

The second part is called the boundary layer dynamics and is the dynamics of the difference between variable  $s$  and variable  $\nu$ . Using the definition  $e = \nu - s$  we rewrite the filter equation (25) as

$$\tau\dot{e} + e = \tau K\nu \quad (27)$$

We now prove the stability of the combined feedback system given by equations (26) and (27).

Consider the following Lyapunov function candidate

$$2V = \rho s^2 + (\mathbf{1} - \rho)e^2$$

Taking the time derivative of the above Lyapunov function along the trajectories of the system given by equations (26) and (27), we obtain

$$\dot{V} = -K\rho s^2 - (1 - \rho)\left(1 - \frac{1}{\tau}\right)e^2 + K(1 - 2\rho)es + \rho s|\Delta\theta||f|$$

where  $\Delta\Theta = \Theta - \hat{\Theta}$ . Since  $f$  is Lipschitz, we obtain

$$\begin{aligned} |\Delta\Theta||f| &\leq l_1|x_1| + l_2|x_2| + l_3|x_3| \\ &\leq \gamma|x_3 + \alpha_2x_2 + \alpha_1x_1| \quad \text{for some } \gamma > 0 \\ &= \gamma|s| \end{aligned}$$

where  $l_1, l_2$  and  $l_3$  are Lipschitz constants. Therefore,

$$\dot{V} \leq -(K + \gamma)\rho s^2 - (1 - \rho)\left(1 - \frac{1}{\tau}\right)e^2 + K(1 - 2\rho)es$$

rearranging the above equation in to a matrix equation, we get,

$$\dot{V} = \begin{bmatrix} s & e \end{bmatrix} \begin{bmatrix} (\gamma - K\rho) & K\frac{(1-2\rho)}{2} \\ K\frac{(1-2\rho)}{2} & (1 - \rho)\left(1 - \frac{1}{\tau}\right) \end{bmatrix} \begin{bmatrix} s \\ e \end{bmatrix}$$

With the appropriate choice of the design parameters  $\rho$ ,  $K$  and  $\tau$ , the above matrix can be made negative definite (diagonally dominant) and thus it is assured that  $s$  and  $e$  go to zero asymptotically.